

# Applications of Pore-Expanded Mesoporous Silica. 1. Removal of Heavy Metal Cations and Organic Pollutants from Wastewater

Abdelhamid Sayari,<sup>\*,†,§</sup> Safia Hamoudi,<sup>‡</sup> and Yong Yang<sup>†</sup>

Centre for Catalysis Research and Innovation (CCRI), Department of Chemistry, University of Ottawa, 10 Marie Curie, Ottawa, Ontario, Canada K1N 6N5, and Department of Chemical Engineering, Laval University, Sainte-Foy, Canada, G1K 7P4

Received September 16, 2004. Revised Manuscript Received October 16, 2004

Postsynthesis pore expansion of as-synthesized MCM-41 silica using *N,N*-dimethyldecylamine affords material **A**, with open pore structure and readily accessible amine groups. The selective removal of the occluded amine gives rise to **B**, a highly porous, hydrophobic material with large surface area and pore volume. Materials **A** and **B** were found to be fast, sensitive, high-capacity recyclable adsorbents for metallic cations and organic pollutants, respectively.

## Introduction

A wide variety of toxic inorganic and organic chemicals are discharged to the environment as industrial wastes, causing serious water, air, and soil pollution. Heavy metals are found in wastewaters originating from chemical manufacturing, painting and coating, mining, extractive metallurgy, nuclear, and other industries.<sup>1,2</sup> Such metals exert a deleterious effect on the fauna and flora of lakes and streams. One of the potential remedies to this problem is the use of adsorption technologies. Activated carbons<sup>3</sup> and a number of low-cost adsorbents such as agricultural residues and peat<sup>4–7</sup> have been used for the removal of heavy metal cations. However, major disadvantages of these adsorbents are their low loading capacities and their relatively weak interactions with metallic cations as evidenced by low metal ion binding constants.<sup>8,9</sup> To overcome this drawback, many investigators developed functionalized adsorbents such as organoclays and surface-modified mesoporous materials. In the case of natural clays, quaternary ammonium compounds and/or thiols have been used to modify clays such as smectite and montmorillonite.<sup>10–13</sup> Mesoporous silicas such as MCM-41,<sup>14–19</sup> HMS,<sup>20,21</sup> SBA-15,<sup>22</sup> and SBA-1<sup>17</sup> have been func-

tionized by various groups to afford materials able to interact strongly with metallic cations, particularly mercury<sup>14–16,20–22</sup> or metallic anions such as chromate and arsenate.<sup>17–19</sup>

With regard to organic pollutants of aquatic ecosystems, phenols are considered priority pollutants since they are harmful to living organisms even at ppb levels. Again, activated carbons are among the most effective adsorbents for organic pollutants in wastewaters, mainly because of their high surface area and their ability to be regenerated by thermal desorption. However, it is common that a substantial fraction of the carbon is lost with each regenerating cycle.<sup>23</sup> In the past few years, there has been increasing interest in developing recyclable inorganic adsorbents, particularly for the efficient removal of organic pollutants from aqueous solutions. For example, organically modified clays<sup>24–28</sup> and layered double hydroxides (LDHs)<sup>29</sup> have drawn much attention as promising adsorbents. Natural clays and LDHs are ion-exchanged often with long chain alkyltrimethylam-

\* Corresponding author. E-mail: abdel.sayari@science.uottawa.ca.

† University of Ottawa.

‡ Laval University.

§ Previously at Laval University.

- (1) Cody, C. A.; Kemnetz, S. J. U.S. Patent 5,667,694, 1997.
- (2) Apak, R.; Tutem, E.; Hugul, M.; Hizal, J. *Water Res.* **1998**, *32*, 430.
- (3) Clifford, D.; Subramonian, S.; Sorg, T. J. *Environ. Sci. Technol.* **1986**, *20*, 1072.
- (4) Al-Asheh, S.; Duvnjak, Z. *Adv. Environ. Res.* **1997**, *1*, 194.
- (5) Wafwoyo, W.; Seo, C. W.; Marshall, W. E. *J. Chem. Technol. Biotechnol.* **1999**, *74*, 1117.
- (6) Suh, J. H.; Kim, D. S. *J. Chem. Technol. Biotechnol.* **2000**, *75*, 279.
- (7) Reddad, Z.; Gerente, C.; Andres, Y.; Le Cloirec, P. *Environ. Sci. Technol.* **2002**, *36*, 2067.
- (8) Mercier, L.; Detellier, C. *Environ. Sci. Technol.* **1995**, *29*, 1318.
- (9) Ravindran, V.; Stevens, M. R.; Badriya, B. N.; Pirbazari, M. *AIChE J.* **1999**, *45*, 1135.
- (10) Greco, C. C. U.S. Patent 5,512,526, 1996.
- (11) Mercier, L.; Pinnavaia, T. J. *Microporous Mesoporous Mater.* **1998**, *20*, 101.
- (12) Celis, R.; Hermosin, M. C.; Cornejo, J. *Environ. Sci. Technol.* **2000**, *34*, 4593.
- (13) Lagadic, I. L.; Mitchell, M. K.; Payne, B. D. *Environ. Sci. Technol.* **2001**, *35*, 984.
- (14) Feng, X.; Fryxell, G. E.; Wang, L.-Q.; Kim, A. Y.; Liu, J. K.; Kemner, M. *Science* **1997**, *276*, 923.
- (15) Liu, J.; Feng, X.; Fryxell, G. E.; Wang, L.-Q.; Kim, A. Y.; Gong, M. *Chem. Eng. Technol.* **1998**, *21*, 97.
- (16) Antochshuk, V.; Olkhovik, O.; Jaroniec, M.; Park, I.-S.; Ryoo, R. *Langmuir* **2003**, *19*, 3031.
- (17) Yoshitake, H.; Yokoi, T.; Tatsumi, T. *Chem. Mater.* **2002**, *14*, 4603.
- (18) Yoshitake, H.; Yokoi, T.; Tatsumi, T. *Chem. Mater.* **2003**, *15*, 1713.
- (19) Fryxell, G. E.; Liu, J.; Hauser, T. A.; Nie, Z.; Ferris, K. F.; Mattigod, S.; Gong, M.; Hallen, R. T. *Chem. Mater.* **1999**, *11*, 2148.
- (20) Mercier, L.; Pinnavaia, T. J. *Environ. Sci. Technol.* **1998**, *32*, 2749.
- (21) Mercier, L.; Pinnavaia, T. J. *Adv. Mater.* **1997**, *9*, 500.
- (22) Liu, M.; Hidajat, K.; Kawi, S.; Zhao, D. Y. *Chem. Commun.* **2000**, *13*, 1145.
- (23) Danis, T. G.; Albanis, T. A.; Petrakis, D. E.; Pomonis, P. J. *Water Res.* **1998**, *32*, 295.
- (24) Mortland, M. M.; Shaobai, S.; Boyd, S. A. *Clays Clay Miner.* **1986**, *34*, 581.
- (25) Boyd, S. A.; Mortland, M. M.; Chiou, C. T. *Soil Sci. Soc. Am. J.* **1988**, *52*, 652.
- (26) Fogler, H. S.; Srinivasan, K. R. U.S. Patent 4,740,488, 1988.
- (27) Huh, J.; Song, D.; Jeon, Y. *Sep. Sci. Technol.* **2000**, *35*, 243.
- (28) Zhao, H.; Vance, G. F. *Water Res.* **1998**, *32*, 3710.
- (29) Zhao, H.; Nagy, K. L. *J. Colloid Interface Sci.* **2004**, *274*, 613.

monium cations or alkylsulfate anions, respectively, to impart them with hydrophobic properties, thus enhancing their sorption capacity for organic contaminants. Similarly, as-synthesized, i.e., surfactant-filled, mesoporous silicas were also used for the adsorption of organic substrates.<sup>30,31</sup> However, materials with filled interlayers (clays and LDHs) or channels (MCM-41 silica) would exhibit low adsorption capacity, and particularly low rates of adsorption because of mass transfer limitation within the crowded space filled with surfactant. Instead of using as-synthesized MCM-41, Inumaru et al.<sup>32,33</sup> used calcined MCM-41 after surface modification through grafting of alkyltriethoxysilane. This allowed the material hydrophobicity to be controlled through the alkyl chain length. Conceivably, the rate of adsorption could also be optimized based on the amount of grafted material. In one example, Hanna et al.<sup>34</sup> prepared a large-pore MCM-41 using trimethylbenzene (TMB) as swelling agent, then removed the TMB by heating in air at 115 °C. This afforded a hydrophobic material with open structure, and thus improved adsorption properties.

Whether dealing with the adsorption of cationic or anionic metal-containing species or with the adsorption of organic pollutants, there is an urgent need to develop novel adsorbents with high surface area and open pore structure for enhanced rate adsorption and increased adsorption capacity. During our quest for pore-size control of mesoporous MCM-41 silica, we developed a novel two-step methodology consisting of (i) synthesis of MCM-41 at relatively low temperature, typically 70–100 °C, then (ii) postsynthesis hydrothermal treatment of the as-synthesized silica mesophase in an aqueous emulsion of long chain *N,N*-dimethyl alkylamine, typically at 120–130 °C for different periods of time.<sup>35–38</sup> Depending on the conditions of both steps, materials with controlled pore sizes from 3.5 up to 25 nm were obtained. The pore volume varied accordingly from typically 0.8 up to 3.6 cm<sup>3</sup>/g, whereas the specific surface areas hardly changed. At least as a working model, it is believed that in the presence of water, the alkylamine self-assembles into an inverted cylindrical micelle inside the alkyltrimethylammonium micelle and is held via attractive hydrophobic forces (Figure 1). This unique organization (material **A**) allows a number of potential applications in environmental remediation and stabilization of metallic and semiconductor nanoparticles to be envisaged. These applications are based on the chemical properties of the expander headgroup and on its high accessibility. Moreover, as shown earlier,<sup>39</sup> the expander can be removed selectively in the presence of ethanol even at room temperature. This affords

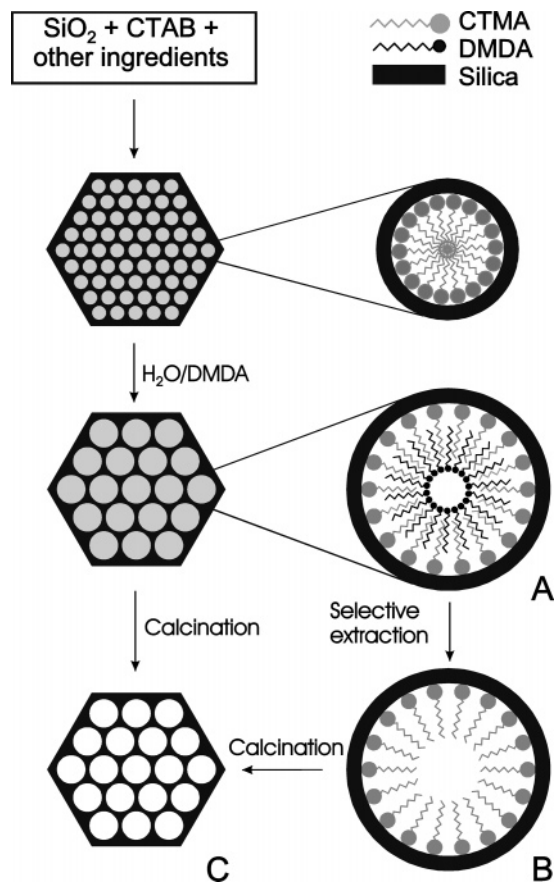


**Figure 1.** Schematic representation of MCM-41 pore-expansion, selective extraction, and calcination.

a high-surface-area mesoporous silica with highly hydrophobic surface and very open pore structure (material **B**).<sup>39</sup> Calcination of material **A** or **B** affords material **C**, a large-pore, high-surface-area mesoporous silica. Similarly to material **A**, materials **B** and **C** could potentially be used in many applications, particularly in catalysis and adsorption/separation processes.

The objective of the current work is to investigate the adsorption properties of (i) the pore-expanded, amine-containing mesoporous silica MCM-41 (i.e., material **A**) toward selected metal cations such as Cu<sup>2+</sup>, Ni<sup>2+</sup> and Co<sup>2+</sup>; and (ii) the pore-expanded, solvent-extracted mesoporous silica MCM-41 (i.e., material **B**) toward typical organic pollutants. Other potential applications for materials **A**, **B**, and **C** will be reported in forthcoming papers.

## Experimental Section

**Material Preparation and Characterization.** The MCM-41 silica to be pore expanded was synthesized using the procedure described earlier.<sup>35,36,40,41</sup> Cab-O-Sil silica (36 g) was mixed with water (60 g) and 25 wt % tetramethylammonium hydroxide (61.56 g). A mixture of 36.5 g of cetyltrimethylammonium bromide (CTAB), 65.52 g of water, and 11.7 g of 30 wt % NH<sub>4</sub>OH was added under vigorous stirring. The mixture composition was 1:0.28:

- (30) Denoyel, R.; Rey, E. S. *Langmuir* **1998**, *14*, 7321.  
 (31) Miyake, Y.; Yumoto, T.; Kitamura, H.; Sugimoto, T. *Phys. Chem. Chem. Phys.* **2002**, *4*, 2680.  
 (32) Inumaru, K.; Kiyoto, J.; Yamanaka, S. *Chem. Commun.* **2000**, 903.  
 (33) Inumaru, K.; Inoue, Y.; Kakii, S.; Nakano, T.; Yamanaka, S. *Phys. Chem. Chem. Phys.* **2004**, *6*, 3133.  
 (34) Hanna, K.; Beurroise, I.; Denoyel, R.; Desplandier-Giscard, D.; Galarmeau, A.; De Renzo, F. J. *Colloid Interface Sci.* **2002**, *252*, 276.  
 (35) Sayari, A.; Kruk, M.; Jaroniec, M.; Moudrakovski, I. L. *Adv. Mater.* **1998**, *10*, 1376.  
 (36) Sayari, A.; Yang, Y.; Kruk, M.; Jaroniec, M. *J. Phys. Chem. B* **1999**, *103*, 3651.  
 (37) Sayari, A. *Angew. Chem., Int. Ed. Engl.* **2000**, *39*, 2920.  
 (38) Kruk, M.; Jaroniec, M.; Sayari, A. *Microporous Mesoporous Mater.* **2000**, *35*, 545.

- (39) Kruk, M.; Jaroniec, M.; Antochshuk, V.; Sayari, A. *J. Phys. Chem. B* **2002**, *106*, 10096.  
 (40) Sayari, A.; Liu, P.; Kruk, M.; Jaroniec, M. *Chem. Mater.* **1997**, *9*, 2499.  
 (41) Kruk, M.; Jaroniec, M.; Sayari, A. *J. Phys. Chem. B* **1999**, *103*, 4590.

0.17:0.17:16.7 SiO<sub>2</sub>/TMAOH/CTAB/NH<sub>3</sub>/H<sub>2</sub>O. After 30 min, the gel was heated in an autoclave at 343 K for 3 days.

Alternatively, the method reported by Sayari and Yang<sup>42</sup> could be used. Tetramethylammonium hydroxide (57.72 g) was added under magnetic stirring in a 700-mL Teflon-lined autoclave containing 556.5 g of distilled water. CTAB (82 g) was added to the solution and stirred until a homogeneous mixture was obtained. Fumed Cab-O-Sil silica (30 g) was slowly added to this mixture, and stirring was maintained for 30 min following the dissolution of silica. The molar composition of the gel was 1:0.32:0.45:67 SiO<sub>2</sub>/TMAOH/CTAB/H<sub>2</sub>O. The vessel was then sealed and placed in an oven at 353 K with no further stirring for 40 h. In both cases, the product was recovered by vacuum filtration and washed repeatedly with distilled, deionized water. It was then dried in ambient conditions.

The pore expansion was achieved through postsynthesis treatment in the presence of *N,N*-dimethyldecylamine (DMDA).<sup>35–38</sup> The as-synthesized surfactant-containing MCM-41 (20 g) was added to an emulsion of DMDA (37 g) in distilled water (411 g) under magnetic stirring. The mixture was stirred for 30 min. Subsequently, the vessel was sealed and placed in an oven at 393 K under static condition for 3 days. The product was recovered by filtration, washed with distilled, deionized water, and dried under ambient conditions.

Nitrogen adsorption experiments were performed at 77 K using a Coulter Omnisorp 100 gas analyzer. Prior to nitrogen adsorption measurements, non-expanded calcined MCM-41 and material **C** were degassed at 200 °C, whereas materials containing surfactants (**A** and **B**) were degassed at room temperature. The specific surface area,  $S_{\text{BET}}$ , was determined from the linear part of the BET plot ( $P/P_0 = 0.05–0.15$ ). The pore size distribution (PSD) was calculated from the adsorption branch using the Kruk, Jaroniec, Sayari (KJS) method.<sup>43</sup> Quantitative elemental analysis of C, H, and N was carried out on a Carlo Erba EA1100 CHNS elemental analyzer.

**Adsorption Measurements.** *Adsorption of Metallic Cations.* Aqueous solutions of Cu, Co, and Ni cations were prepared by dissolving the corresponding nitrates in double-distilled water. Adsorption assays were performed batchwise in 250-mL Erlenmeyer flasks. Different concentrations and volumes of the relevant metal solutions were added to 0.25-g batches of the adsorbent under vigorous stirring at room temperature. The stirring continued for 60 min before the slurries were filtered, and the obtained solutions were analyzed by atomic absorption spectroscopy using standard solutions to calibrate the instrument.

The amount of metal retained in the sorbent phase (mg/g) was calculated by

$$q_e = (C_i - C_e)V/m$$

where  $C_i$  and  $C_e$  are the initial and final (equilibrium) concentrations of the metal ions in solution (mg/L),  $V$  is the solution volume (L), and  $m$  is the mass of sorbent (g). The solid/water distribution ratios of metals were calculated by

$$K_D = [(C_i - C_e)/C_e] \times [V/m]$$

Since the long chain alkylamine is withheld by electrostatic forces, it is essential to investigate the stability of the adsorbent and its regeneration. To this end, consecutive adsorption–desorption cycles were performed using a Cu<sup>2+</sup> containing solution and the same adsorbent batch. After contacting the fresh adsorbent with a

copper solution of 0.004 M, it was separated, washed, and dried at room temperature. The now copper-loaded sample was then stirred in 200 mL of HNO<sub>3</sub> solution (pH = 3) for 30 min at room temperature to strip the Cu<sup>2+</sup> cations.<sup>44</sup> After filtration and washing, the sample was neutralized to pH = 7 and dried. This first adsorption–desorption cycle was followed by three other cycles using the same adsorbent batch. At this stage, the solid material was contacted with an emulsion of *N,N*-dimethyloctylamine (DMOA), and tested again for the adsorption of copper cations.

*Adsorption of Organic Pollutants.* Two typical organic pollutants, namely 4-chloroguaiacol (i.e., 4-chloro-2-methoxyphenol) and 2,6-dinitrophenol were used. Several aqueous solutions with different concentrations were prepared. Material **B** (0.25 g) was contacted with 50 mL of solution. After stirring for a period of 60 min, the slurry was allowed to decant for 60 min, then an aliquot of solution was withdrawn for analysis. To the slurry, 50 mL of fresh solution was added and the sequence of stirring–decantation was repeated. Additional cycles were performed until the material was saturated with the organic pollutant; i.e., when the concentration of the supernatant liquid was stable. The concentration of pollutants was determined by HPLC using a 510 Waters system equipped with a 490E UV–Vis detector and C18  $\mu$ Bondapak column. The mobile phase was 85:15 v/v methanol/water for chloroguaiacol and 59:40:1 methanol/water/acetic acid for dinitrophenol. The detector was set at 254 and 270 nm for dinitrophenol and chloroguaiacol, respectively.

## Results and Discussion

Figure 2 shows the nitrogen adsorption–desorption isotherms and the corresponding pore size distributions (PSDs) for materials **A**, **B**, and **C** as well as the nonexpanded, calcined MCM-41 silica. The BET surface area, pore size, and pore volume are given in Table 1. The nonexpanded calcined sample exhibited a reversible adsorption–desorption isotherm with the characteristic nitrogen condensation–evaporation step at a relative pressure of ca. 0.3. As shown in Figure 2b, the corresponding PSD was very narrow. As expected, material **C** exhibited highly enlarged pores with relatively narrow size distribution with an average diameter of 11 nm. The pore volume also increased by a factor of ca. 3 and the surface area remained very high. Material **B**, which contained about 50 wt % of cetyltrimethylammonium (CTMA) surfactant, also exhibited a wide open pore structure, particularly suitable for fast adsorption of hydrophobic molecules. Material **A** which contains both surfactants, i.e., CTMA and DMDA, seems to have low pore volume (0.2 cm<sup>3</sup>/g), low surface area (89 m<sup>2</sup>/g), and a broad PSD. However, taking into consideration that such a material contains ca. 25 w% CTMA and ca. 50 w% DMDA, the pore volume would actually be about 0.8 cm<sup>3</sup> per gram of silica. Assuming an ideal situation where (i) materials **B** and **C** contain perfectly cylindrical pores with pore volumes of 0.8 and 2.6 cm<sup>3</sup> per gram of silica, respectively, and (ii) no shrinkage takes place during calcination of **A** or **B** into **C**, an average pore diameter of  $d_B = 6.1$  nm for material **B** could be calculated using  $d_B = d_C(V_B/V_C)^{1/2}$ . This indicates that, based on the schematic representation shown in Figure 1, material **A** exhibits wide hydrophilic channels that allow

(42) Sayari, A.; Yang, Y. *J. Phys. Chem. B* **2000**, *104*, 4835.

(43) Kruk, M.; Jaroniec, M.; Sayari, A. *Langmuir* **1997**, *13*, 6267.

(44) Dai, S.; Burleigh, M. C.; Shin, Y.; Morrow, C. C.; Barnes, C. E.; Xue, Z. *Angew. Chem., Int. Ed.* **1999**, *38*, 1235.



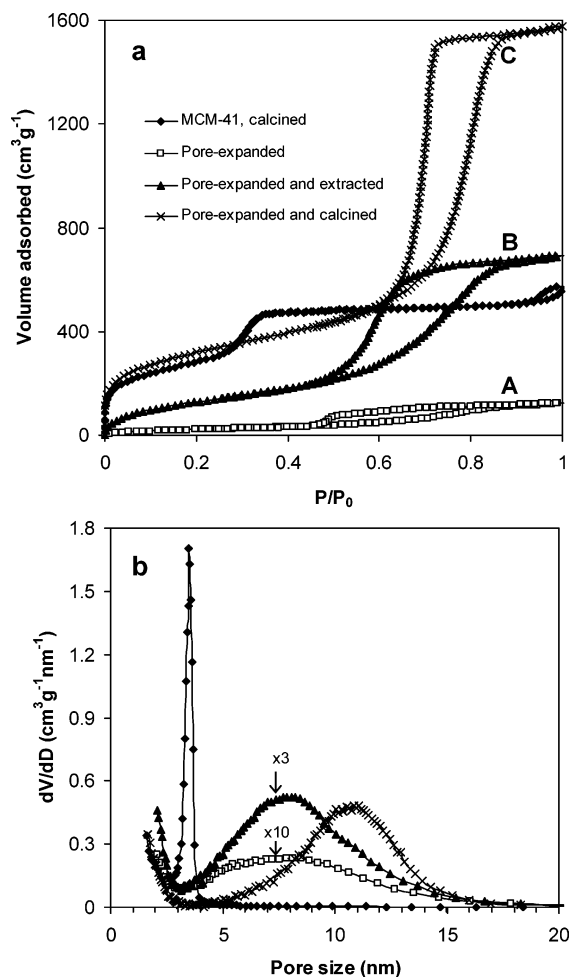


**Figure 2.** (a) Nitrogen adsorption–desorption isotherms for (◆) calcined MCM-41; (□) pore-expanded MCM-41 (material A in text); (▲) pore-expanded, selectively extracted MCM-41 (material B); (×) pore-expanded, calcined MCM-41 (material C); and (b) the corresponding pore size distributions.

**Table 1. Structure Properties of Pore-expanded MCM-41**

sample <sup>a</sup>	surface area (m <sup>2</sup> /g)	pore size (nm)	pore volume (cm <sup>3</sup> /g)
MCM-41	1025	3.5	0.87
A	89		0.20
B	509	8.5	1.08
C	1192	11.0	2.60

<sup>a</sup> See Figure 1.

**Table 2. Co(II) Adsorption on Material A**

solution/adsorbent (mL/g)	Co <sup>2+</sup> (mg/L)		% removal	adsorbed amount (mg/g)	$K_d \times 10^{-2}$
	initial	final			
160	1178	830	29.54	55.68	0.7
120	1178	662	43.75	61.85	0.9
80	1178	540	54.16	51.04	0.9
160	235.6	69	70.58	26.60	3.9
120	235.6	66	71.98	20.35	3.1
200	47.1	2.4	94.91	8.94	37.3
200	9.4	0.1	98.94	9.40	186

the transport of water-soluble species such as metallic cations with little or no resistance, which in turn increases their rate of interaction with the DMDA amine headgroups.

**Adsorption of Metallic Cations.** Data for the adsorption of Co<sup>2+</sup>, Ni<sup>2+</sup>, and Cu<sup>2+</sup> are shown in Tables 2–4. As shown the adsorption capacity was high and, depending on the nature of the metal, it varied between 50 and more than 100

**Table 3. Ni(II) Adsorption on Material A**

solution/adsorbent (mL/g)	Ni <sup>2+</sup> (mg/L)		% removal	adsorbed amount (mg/g)	$K_d \times 10^{-2}$
	initial	final			
80	5870	5189	11.60	54.47	0.5
160	1174	841	28.34	53.23	1.6
120	1174	820	30.14	42.46	1.7
80	1174	660	43.75	41.09	3.1
160	234.8	81	65.37	24.56	7.5
120	234.8	69	70.57	19.89	9.6
200	47	3.29	92.99	8.73	53.1
200	9.4	0.77	91.80	1.72	44.8
200	1.9	0.16	91.48	0.34	43.0

**Table 4. Cu(II) Adsorption on Material A**

solution/adsorbent (mL/g)	Cu <sup>2+</sup> (mg/L)		% removal	adsorbed amount (mg/g)	$K_d \times 10^{-2}$
	initial	final			
80	6350	5062	20.2	103	0.2
160	1270	604	52.4	106	1.8
120	1270	393	69.1	105	2.7
80	1270	69	94.6	96	14.0
160	254	10.67	95.8	38.93	36.5
120	254	9.14	96.4	29.38	32.1
200	254	1.50	99.4	50.50	337
200	50.8	0.35	99.3	10.10	288
200	10.16	0.08	99.3	2.02	269
200	2.03	0.05	97.5	0.40	79.3
100 <sup>a</sup>	63.80	0.26	99.6	6.38	260

<sup>a</sup> Reference 44.

**Table 5. Cu(II) Adsorption: Cycling and Regeneration of the Adsorbent**

cycle	solution/adsorbent (mL/g)	Cu <sup>2+</sup> (mg/L)		% removal	adsorbed amount (mg/g)	$K_d \times 10^{-2}$
		initial	final			
1	200	254	1.5	99.41	50.50	337
2	200	254	208	18.11	20.91	1
3	200	254	219	13.78	19.50	0.9
4	200	254	243	4.13	7.42	0.3
5 <sup>a</sup>	200	254	10	96.06	48.80	4.9

<sup>a</sup> Cycle 5 was performed on DMOA-reloaded adsorbent.

mg per g of adsorbent. Though no kinetic measurements were made yet, the adsorption of all cations was very fast. For comparison, the results obtained by Dai et al.<sup>44</sup> for the adsorption of copper cations using an imprint-coated mesoporous silica are included in Table 4. Experiments using very dilute solutions, i.e., 10 ppm or less, indicate that in all cases 90–99.3% of cations were removed, indicating the high sensitivity of the current adsorbent to such metallic cations.

The results for the cycling and regeneration of the adsorbent are shown in Table 5. As seen, the adsorbed amount of copper decreased continuously from 50 mg/g for the first cycle to 7 mg/g for the fourth one. This is due to progressive loss of amine during the acid treatment to release the metallic cations. Under acidic pH, the amine protonates, its affinity to water increases and it is partly displaced into the aqueous phase. This was directly evidenced by elemental analysis, as the C to N ratio in the material after 4 adsorption cycles was 17.5, almost the same as in CTMA (i.e., 19), indicating that hardly any DMDA remained in the solid material. However, treatment with DMOA gave rise to a significant decrease in the C to N ratio to ca. 13, indicative of the high adsorption capacity of the hydrophobic (DMDA depleted) material toward organic molecules such as DMOA. As seen, the initial adsorption capacity of material A toward copper cations was almost fully restored.

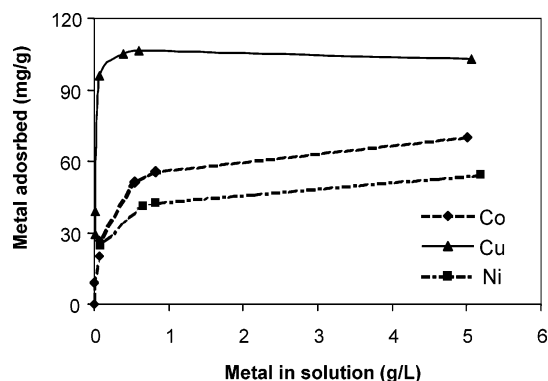


Figure 3. Adsorption isotherms for Co, Cu, and Ni cations on material A.

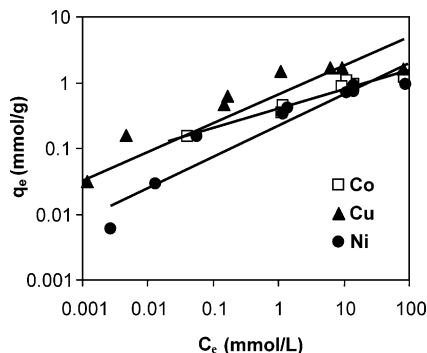


Figure 4. Adsorption isotherms according to the Freundlich model (symbols, experimental data; lines, predicted data).

This work provides clear evidence that, because of its unique structure, material **A** is a fast, high-capacity adsorbent for numerous metallic cations. It also can be fully regenerated by simple mixing with an alkylamine. Moreover, as shown here, a different amine than the original DMDA could be used possibly to achieve higher loading, thus higher initial adsorption capacity. Organic molecules with other functionalities can also be used. For example, it is conceivable to load alkylthiols for more efficient adsorption of metallic cations such as  $\text{Pb}^{2+}$ ,  $\text{Zn}^{2+}$ ,  $\text{Cd}^{2+}$ , and  $\text{Hg}^{2+}$ .

Figure 3 shows the adsorption isotherms of the three metallic cations investigated. These isotherms are relatively well described using the Freundlich adsorption model as depicted in Figure 4. The Freundlich constants  $k$  and  $1/n$  together with the saturation capacities ( $q_s$ ) are presented in Table 6. The constant  $k$  which is related to the sorption capacity<sup>4</sup> indicates that the order of the sorption affinity of the three substrates to material **A** is as follows:  $\text{Cu} > \text{Co} > \text{Ni}$ .

**Adsorption of Organic Pollutants.** Using material **B** and solutions with different initial concentrations of 4-chloroguaiacol or 2,6-dinitrophenol, the adsorption data shown in Table 7 were obtained. As expected, within experimental

Table 6. Freundlich<sup>a</sup> Isotherm Constants

metal cation	$k$ (mmol/g)	$1/n$ (L/g)	$q_s^b$ (mmol/g)
Cu	0.9465	0.5182	1.62
Co	0.4667	0.4676	1.18
Ni	0.2312	0.2232	0.93

<sup>a</sup> Freundlich linearized model:  $\text{Ln}(q_e) = \text{Ln}(k) + (1/n)\text{Ln}(C_e)$ . <sup>b</sup> Subscript  $s$  refers to saturation capacity.

Table 7. Adsorption of Chloroguaiacol and Dinitrophenol on Material B

pollutant	concentration (g/L)	% adsorbed pollutant <sup>a</sup>	adsorbent capacity (mg/g)
chloroguaiacol	0.11	89.3	96.6
chloroguaiacol	0.25	89.9	95.6
chloroguaiacol	0.50	19.9	95.2
dinitrophenol	0.08	98.7	115.5
dinitrophenol	0.25	98.5	88.6
dinitrophenol <sup>b</sup>		86	40
2-chlorophenol <sup>c</sup>	0.1	96.9	3.1
phenol <sup>d</sup>	4	30.0	45.0

<sup>a</sup> In the first cycle. <sup>b</sup> Reference 46; capacity is given in  $\text{mg}/\text{cm}^3$ . <sup>c</sup> Reference 45. <sup>d</sup> Reference 27.

errors, the adsorption capacity was independent of the initial concentration of the pollutant solutions. The capacity was quite high for both substances, reaching 95 and 110  $\text{mg}/\text{g}$  for 4-chloroguaiacol and 2–6-dinitrophenol, respectively. As shown in Table 7, these numbers compare favorably with the adsorption capacity of other adsorbents such as bituminous shale,<sup>45</sup> cyclodextrins,<sup>46</sup> and organically modified montmorillonite.<sup>27</sup>

Owing to the open pore structure of material **B**, the adsorption is particularly fast. Moreover, the adsorbed pollutants may be easily stripped using appropriate solvents and the adsorbent may thus be reused.

In conclusion, this work describes two novel and structurally related nanoporous adsorbents for the removal of metallic cations and organic pollutants, respectively. Because of their open pore structure and their suitable surface properties, these materials are fast, high-capacity adsorbents. Their adsorption efficiency remains high even in the presence of very dilute solutions of adsorbate. Moreover, in both cases the adsorbents can be easily regenerated through acid or solvent washing.

**Acknowledgment.** A.S. is Government of Canada Research Chair in *Catalysis using Nanostructured Materials*. We thank the Natural Sciences and Engineering Research Council (NSERC) and the Canada Foundation for Innovation (CFI) for financial support. S.H. is grateful to NSERC for a postdoctoral fellowship.

CM048393E

(45) Tutem, E.; Apak, R.; Unal, C. F. *Water Res.* **1998**, *32*, 2315.

(46) Ma, M.; Li, D. *Chem. Mater.* **1999**, *11*, 872.